Journal of the Neurological Sciences 378 (2017) 110–119

Contents lists available at ScienceDirect

Journal of the Neurological Sciences

journal homepage: www.elsevier.com/locate/jns

The anteroposterior and primary-to-posterior limbic ratios as MRI-derived volumetric markers of Alzheimer's disease

Adolfo Jiménez-Huete [a,*], Susana Estévez-Santé [b], for the ADNI group [1]

[a] Department of Neurology, Hospital Ruber Internacional, C/La Masó, 38, 28034 Madrid, Spain
[b] Department of Neurology, Hospital Universitario Príncipe de Asturias, Alcalá de Henares, Spain

ARTICLE INFO

Article history:
Received 25 January 2017
Received in revised form 17 April 2017
Accepted 26 April 2017
Available online 27 April 2017

Keywords:
Alzheimer disease (MeSH)
Mild cognitive impairment
Magnetic resonance imaging (MeSH)
Volumetry

ABSTRACT

Background/aims: Alzheimer's disease (AD) shows a characteristic pattern of brain atrophy, with predominant involvement of posterior limbic structures, and relative preservation of rostral limbic and primary cortical regions. We aimed to investigate the diagnostic utility of two gray matter volume ratios based on this pattern, and to develop a fully automated method to calculate them from unprocessed MRI files.
Patients and methods: Cross-sectional study of 118 subjects from the ADNI database, including normal controls and patients with mild cognitive impairment (MCI) and AD. Clinical variables and 3 T T1-weighted MRI files were analyzed. Regional gray matter and total intracranial volumes were calculated with a shell script (gm_extractor) based on FSL. Anteroposterior and primary-to-posterior limbic ratios (APL and PPL) were calculated from these values. Diagnostic utility of variables was tested in logistic regression models using Bayesian model averaging for variable selection. External validity was evaluated with bootstrap sampling and a test set of 60 subjects.
Results: gm_extractor showed high test-retest reliability and high concurrent validity with FSL's FIRST. Volumetric measurements agreed with the expected anatomical pattern associated with AD. APL and PPL ratios were significantly different between groups, and were selected instead of hippocampal and entorhinal volumes to differentiate normal from MCI or cognitively impaired (MCI plus AD) subjects.
Conclusion: APL and PPL ratios may be useful components of models aimed to differentiate normal subjects from patients with MCI or AD. These values, and other gray matter volumes, may be reliably calculated with gm_extractor.

1. Introduction

Alzheimer's disease (AD) is the most prevalent cause of dementia in the western world [1]. Defeating AD and other dementias has been established as a priority for European science and society [2]. The pathologic hallmarks of AD include a combination of neuronal loss, glial proliferation, beta-amyloid neuritic plaques, and tau-laden neurofibrillary tangles [3]. The distribution of brain lesions in AD is not uniform. Existing evidence points to a major involvement of the posterior limbic system, including the hippocampus, the entorhinal cortex, the posterior cingulate cortex, and the multimodal associative temporoparietal areas [4–7]. In contrast, the primary motor, sensory and visual areas, and the rostral limbic system, including the anterior cingulate and frontal ventromedial regions, seem to be relatively spared [4,8,7]. This selective anatomical pattern in AD opens the way to the development of structural and functional biomarkers. To date, the volumes of the hippocampus and the entorhinal cortex have been the most frequently used volumetric measures for the diagnosis of AD (reviewed at [9]). These volumes have been shown to discriminate normal subjects from patients with amnestic mild cognitive impairment (MCI) or AD [9], and to predict the progression from MCI to AD, especially when tested longitudinally [10–12].

In this study we have further explored the use of MRI-derived brain volumetric measures for the diagnosis of AD. In particular, we have developed and tested the diagnostic utility of two volume ratios aimed to detect the anatomical pattern associated with AD: 1) the anteroposterior limbic ratio (APL), which compares the gray matter volumes of the anterior and posterior limbic structures, and 2) the primary-to-posterior limbic ratio (PPL), which compares the gray matter volumes of the primary motor, sensory and visual areas, and the posterior limbic structures. The use of volume ratios is theoretically appealing, as they avoid the need to normalize by head size and may be less

* Corresponding author.
E-mail address: ajimenez@ruberinternacional.es (A. Jiménez-Huete).

[1] Data used in preparation of this article were obtained from the Alzheimer's Disease Neuroimaging Initiative (ADNI) database (adni.loni.usc.edu). As such, the investigators within the ADNI contributed to the design and implementation of ADNI and/or provided data but did not participate in analysis or writing of this report. A complete listing of ADNI investigators can be found at: http://adni.loni.usc.edu/wp-content/uploads/how_to_apply/ADNI_Acknowledgement_List.pdf.

http://dx.doi.org/10.1016/j.jns.2017.04.046
0022-510X/

sensitive to technical variability. The study population was collected from the Alzheimer's Disease Neuroimaging Initiative (ADNI) database (adni.loni.usc.edu), and included cognitively intact elderly subjects, and patients with amnestic MCI and AD. A cross-sectional design was applied with the main objective of identifying the best volumetric variables to differentiate the clinical groups among the APL and PPL ratios and the gray matter volumes of 11 regions.

In order to facilitate clinical use, brain volumes were calculated with a fully automated method wrapped in a shell script (gm_extractor). This script takes a T1-weighted MRI in NIfTI format as input, and gives a series of global and regional volumes and processed images as output. gm_extractor applies a pipeline of free-software tools, mainly based on the FSL suite [13], and it is also freely available (see link below).

2. Patients and methods

2.1. Selection of the study population

Data used in the preparation of this article were obtained from the ADNI database (adni.loni.usc.edu). The ADNI was launched in 2003 as a public-private partnership, led by Principal Investigator Michael W. Weiner, MD. The primary goal of ADNI has been to test whether serial MRI, positron emission tomography, other biological markers, and clinical and neuropsychological assessment can be combined to measure the progression of MCI and early AD. For up-to-date information, see www.adni-info.org.

In this work we opted to perform a transversal (cross-sectional) analysis, and to focus on high resolution (3 Tesla) images in order to optimize the segmentation step. To this end the patients were collected from the ADNI database using the advanced search machine and selecting the following options: ADNI screening or baseline visits, 3 Tesla MRI, T1-weighted images, and original (unprocessed) files. There were 118 subjects fulfilling these criteria, who were categorized into three clinical groups: normal, MCI (including cases labeled as MCI, early MCI or late MCI), and AD. Of note, the MCI patients correspond to the amnestic MCI subtype of more recent classifications [14]. Age, gender, years of education, and Mini-mental State Examination (MMSE) and Functional Activities Questionnaire (FAQ) scores were also registered. Due to the limited size of the main sample, a test set of 60 subjects (20 per group) was also analyzed and used for external validation. These cases were selected from the META3MRI list of the ADNI database.

2.2. Pipeline of brain MRI analysis

The initial brain MRI files were the original MPRAGE (T1-weighted) files downloaded from ADNI. The technical details of the MRI sequences and protocols can be reviewed at http://adni.loni.usc.edu/about/centers-cores/mri-core/. Conversion from DICOM to NIfTI was performed with dcm2nii (http://people.cas.sc.edu/rorden/mricron).

The gray matter volumes of 11 brain regions, the total intracranial volume (TIV), and the total gray and white matter brain volumes were calculated with a fully automated method wrapped in a bash script (gm_extractor). gm_extractor contains a pipeline based on the FSL suite version 5.0.9 [13], the optiBET brain extraction program [15], and the mat2det matrix-to-determinant program (http://enigma.usc.edu/). It also requires 11 binary brain masks, which were created by applying fslmaths to the corresponding Harvard-Oxford probabilistic maps included in FSL with a threshold of 30. This threshold was empirically selected after visual inspection of the effects of a range of values (1, 10, 30, 50, 70, 100) on the hippocampal mask. In particular, low thresholds led to the unintended inclusion of the amygdala and the parahippocampal gyrus, whilst high thresholds led to the exclusion of significant portions of the hippocampal gray matter. In addition to the hippocampus, we analyzed the following cortical regions: frontal pole, frontal ventromedial cortex, temporal pole, parahippocampal gyrus (anterior division), cingulate gyrus (anterior division), cingulate gyrus (posterior division), precentral gyrus, postcentral gyrus, precuneus cortex, and intracalcarine cortex. The parahippocampal gyrus (anterior division) of the Harvard-Oxford atlas mainly corresponds to the entorhinal cortex.

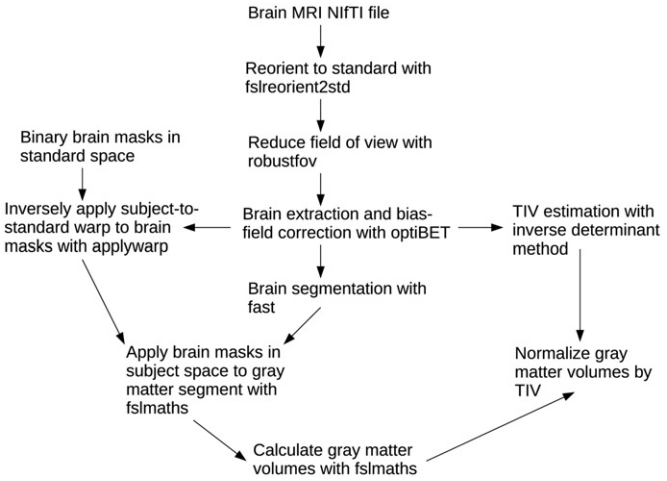

Fig. 1. Pipeline of brain MRI analysis. TIV: total intracranial volume.

The pipeline in gm_extractor included the following steps (Fig. 1): 1). The original NIfTI files were reoriented to standard with fslreorient2std. 2) The field of view was cropped to reduce neck tissue with FSL's robusfov. 3). The resulting image was brain extracted with optiBET. optiBET includes an initial brain extraction step with bias-field correction, and subsequent linear and non-linear registrations. optiBET requires two minor modifications in order to run within gm_extractor: add “cp ${i}_step5.nii.gz my_inverted_warp.nii.gz” at the end of step 5, and save the file as optiBET_2.sh. The inclusion of optiBET instead of BET was an essential step to obtain a fully automated method. 4). The subject-to-standard warp file obtained with optiBET was inversely applied to the binary brain masks with FSL's applywarp. 5). The brain image was segmented into gray matter, white matter, and cerebrospinal fluid with FSL's fast. 6). The binary masks in subject space were applied to the gray matter segment (pve_1) with fslmaths, obtaining 11 gray matter extracted regions. 7). The volumes of gray matter were calculated with fslmaths. 8). TIV was estimated with the inverse determinant method according to the Enigma protocol (http://enigma.ini.usc.edu/protocols/imaging-protocols/protocol-for-brain-and-intracranial-volumes/). The details of the processing steps may be directly reviewed opening the annotated code with a text editor such as gedit. The shell script (gm_extractor) and the brain masks can be both freely accessed at a web link (see footnote[2]). Correct execution of the pipeline was evaluated through visual inspection of the intermediate files with fslview. Failures in the procedure were registered, but no manual interventions were allowed. All analyses were done with a home computer with the following specifications: CPU: i7-6500 U, 2.5 GHz. RAM: 16 GB. Hard disk: 480 GB SSD. Operating System: Ubuntu Linux 16.04.1LTS (64 bits).

2.3. Statistical methods

Statistical analyses were performed with R version 3.3.2 [16]. Differences between groups in demographic and neuropsychological variables were analyzed with one-way analysis of variance (ANOVA) or the Pearson's Chi-Square test.

Test-retest reliability of gm_extractor was analyzed in a subset of 30 cases, which included patients of the three groups in a similar

[2] https://www.dropbox.com/sh/i0j8gpvy5c83m58/AAAjaGsMNb8LZ5jX3ddrQy1ba?dl=0

proportion to that of the whole sample. To this end, the volumes obtained from the initial MRI and a second MRI performed shortly after, were compared with the Pearson's correlation coefficient. Concurrent validity of the hippocampal volumes obtained with gm_extractor was explored by comparing these values to those obtained with SNT and FIRST. FIRST is a fully automated program included in FSL [17]. We used the command-line version (first) with default options. SNT is a semi-automated method that has shown excellent correlation with manual measures (Medtronic Surgical Navigation Technologies, Louisville, CO) [18]. SNT volumes were directly downloaded from the ADNI database, and were available for 88 of 118 patients. FIRST failed in two cases, remaining 86 patients for comparison. The three methods were compared with the Pearson's correlation coefficient and Bland-Altman plots.

Brain volumes obtained with gm_extractor were normalized to TIV according to this formula: Normalized volume = (Volume/TIV) * 10,000 [19]. From the regional volumes we calculated two ratios designed to detect the anatomical pattern typical of AD: 1) APL ratio = (Frontal ventromedial + Cingulate anterior) / (Hippocampus + Parahippocampus anterior + Cingulate posterior + Precuneus), and 2) PPL ratio = (Precentral gyrus + Postcentral gyrus + Intracalcarine gyrus) / (Hippocampus + Parahippocampus anterior + Cingulate posterior + Precuneus). The formulae of the APL and PPL ratios were designed in order to obtain values that increased with disease progression (i.e. higher values represent more advanced stages of disease). Normalized volumes and volume ratios were compared between groups with analysis of covariance (ANCOVA), taking age, gender, and years of education as covariates. Adjusted P values <0.05 in the likelihood ratio test were considered as significant. Post-hoc tests comparing two-by-two the clinical groups were performed with the Tukey's Honest Significant Difference test, and were only applied when the ANCOVA test was significant.

In order to evaluate the diagnostic utility of the volumetric variables, four logistic regression models aimed to differentiate normal from MCI, normal from AD, normal from cognitively impaired (MCI plus AD), and MCI from AD patients were constructed. In a first step, Bayesian model averaging (BMA) was used to select the best volumetric variables among the 11 regional gray matter volumes and the two ratios (APL and PPL) [20]. Of note, BMA is mainly a predictive method for variable selection, which primes the accuracy of the final models over their logical structure. In a second step, age, gender and years of education were added to the volumetric variables, and a sequential method of variable elimination with the likelihood ratio test was applied. Relative quality of the models was evaluated with the Akaike's Information Criterion (AIC). Diagnostic accuracy of models was analyzed with the OptimalCutpoints package using the receiver operating characteristic curve (ROC) method [21]. The external validity of the models was tested with both bootstrap sampling and the holdout method (training versus test sets). Bootstrap 95% confidence intervals of the areas under the ROC curves (AUC) were estimated with the boot package applying the percentile method and 1000 replications [22]. The accuracy of the classification of the test set was analyzed with the same methods used to evaluate the main (training) sample.

3. Results

3.1. Performance, test-retest reliability and concurrent validity of gm_extractor

Visual inspection of the reoriented, cropped and brain-extracted images and the registered brain masks showed anatomically correct results in 117 of 118 cases (99.2%). The pipeline wrapped in gm_extractor failed in one of 118 patients (0.8%). This problem could be solved by changing the cropping step, but the case was excluded to avoid any kind of manual intervention. Processing time for each subject was 16–18 min.

Test-retest correlation coefficients of brain volumes calculated with gm_extractor were all high ($r > 0.9$): TIV: 0.999. Total gray matter: 0.944. Total white matter: 0.929. Frontal pole: 0.970. Frontal ventromedial cortex: 0.972. Temporal pole: 0.976. Hippocampus: 0.995. Parahippocampal gyrus (anterior division): 0.984. Cingulate gyrus (anterior division): 0.993. Cingulate gyrus (posterior division): 0.994. Precentral gyrus: 0.981. Postcentral gyrus: 0.989. Precuneus cortex: 0.951. Intracalcarine cortex: 0.980. APL ratio: 0.992. PPL ratio: 0.984.

Comparison of hippocampal volumes (in mL) calculated with gm_extractor, FIRST and SNT is shown in Fig. 2. Pearson's correlation coefficients between gm_extractor and the other methods were both high (gm_extractor vs. FIRST = 0.841, gm_extractor vs. SNT = 0.862). Bland-Altman plots showed that gm_extractor gave slightly lower values on average to those obtained with FIRST (mean difference = −0.285, standard deviation (SD) of differences = 0.699), but markedly higher values than those obtained with SNT (mean difference = 2.603, SD of differences = 0.539).

3.2. Descriptive and bivariate analyses of the demographic, clinical and volumetric variables

The demographic and clinical characteristics of the patients are summarized in Table 1. As expected, there were marked differences between groups in the MMSE and FAQ scores. The three groups also showed significant differences in gender and years of education, but not in age.

The normalized volumes and the two volume ratios (APL and PPL) of the three groups are summarized in Table 2. Gray matter volumes of posterior limbic structures showed progressively decreasing values in the three groups: normal > MCI > AD (Fig. 3). Due to the way in which they were codified, this sequence was inverted for the APL and PPL ratios (Fig. 3). Differences between groups in the volumes of the posterior limbic structures and the APL and PPL ratios were statistically significant in tests adjusted for age, gender and years of education. In contrast, gray matter volumes of primary motor, sensory and visual areas, and anterior limbic structures (anterior cingulate, frontal ventromedial) were similar in the three groups (Fig. 4). The adjusted P values for these variables were all higher than 0.05.

3.3. Construction and diagnostic accuracy of the logistic regression models

The selection of the volumetric variables using BMA showed different results according to the clinical context. The variables selected to differentiate normal from MCI patients were the anterior cingulate volume (posterior probability = 0.343) and the APL ratio (0.434). The same two variables were selected to differentiate normal from cognitively impaired subjects (MCI plus AD). The posterior probabilities in this case were 0.453 and 0.558, respectively. In contrast, the variables selected to differentiate normal from AD patients were the hippocampus (0.618), the postcentral gyrus (0.301), and the PPL ratio (0.544). The best variable to distinguish MCI from AD was the PPL ratio (0.249), but in this context all variables showed low to moderate posterior probabilities.

The addition of age, gender and years of education to the previously selected volumetric variables, and the subsequent elimination of the non-significant variables with the likelihood ratio test, led to the four final logistic regression models shown in Table 3. The diagnostic accuracy of the models is summarized in Table 4, and their ROC curves are depicted in Fig. 5. The model aimed to differentiate normal from AD subjects was the most accurate (AUC = 0.933). In contrast, the MCI vs. AD model was inaccurate (AUC = 0.620). The other two models (normal vs. MCI, and normal vs. cognitively impaired) showed intermediate values (AUC = 0.830 and 0.833).

For the sake of comparison, we also calculated the accuracy of hippocampal gray matter volume to differentiate normal subjects from patients with MCI or cognitive impairment (MCI plus AD). The

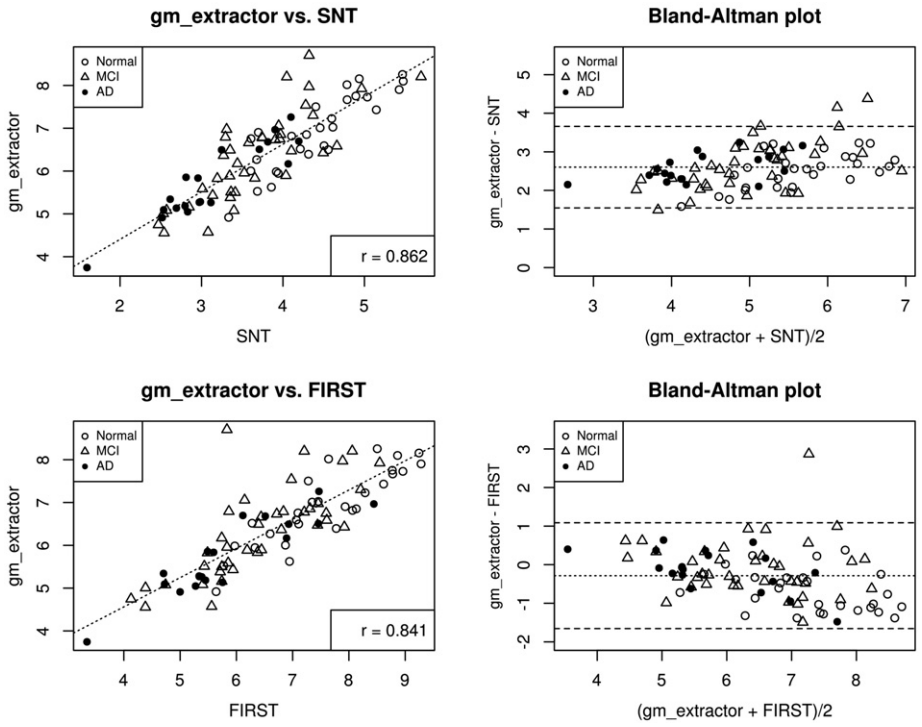

Fig. 2. Comparison of the hippocampal volumes in mL calculated with gm_extractor and SNT (upper row) or FIRST (lower row). Left panels are scatter plots with linear regression lines. Right panels are Bland-Altman plots, where the dotted lines represent the mean difference between methods, and the dashed lines correspond to the limits of agreement (±1.96 * standard deviation of differences).

coefficients and accuracy of the hippocampal models were as follows: 1) Normal vs. MCI: Constant = 6.795 (Standard error (SE) = 1.926). Hippocampus = −0.138 (SE = 0.041, P < 0.001). AIC = 114.511. AUC = 0.711. Sensitivity = 0.796. Specificity = 0.553. 2) Normal vs. Cognitively impaired (MCI plus AD): Constant = 7.953 (SE = 1.804). Hippocampus = −0.156 (SE = 0.038, P < 0.001). AIC = 130.146. AUC = 0.749. Sensitivity = 0.658. Specificity = 0.684. Of note, the four models selected with BMA all contained the hippocampal gray matter volume either by itself or within the composite APL and PPL ratios.

3.4. External validity of the logistic regression models

Bootstrap 95% confidence intervals of the AUCs are shown in Table 4. The test set included 60 subjects (20 per group: normal, MCI, AD) with a

Table 1
Demographic and clinical characteristics of the patients according to clinical group (normal controls, mild cognitive impairment (MCI), and Alzheimer's disease (AD)).

	Normal (n = 38)	MCI (n = 54)	AD (n = 25)	P
Age				
Mean (SD)[a]	74.9 (4.5)	74.1 (8.1)	73.8 (8.2)	0.818
Gender				
Female	23 (60.5%)	20 (37%)	17 (68%)	0.014
Male	15 (39.5%)	34 (63%)	8 (32%)	N[b]-MCI 0.044 N-AD 0.049 MCI-AD 0.020
Education yrs.				
Mean (SD)	16.1 (2.8)	15.4 (3.2)	14.0 (3.3)	0.042 N-MCI 0.575 N-AD 0.033 MCI-AD 0.170
MMSE[c]				
Mean (SD)	29.3 (0.8)	26.9 (1.9)	23.1 (2.2)	<0.001 N-MCI <0.001 N-AD <0.001 MCI-AD <0.001
FAQ[d]				
Median (IQR)[e]	0 (0)	2 (5.75)	10 (6)	<0.001 N-MCI <0.001 N-AD <0.001 MCI-AD <0.001

[a] Standard deviation.
[b] Normal subjects.
[c] Mini-mental State Examination.
[d] Functional Activities Questionnaire.
[e] Interquartile range.

Table 2
Brain volumetric measurements of the patients according to clinical group. The values correspond to the mean and standard deviation of the volumes normalized by total intracranial volume (see text for details).

	Normal (n = 38)	MCI (n = 54)	AD (n = 25)	P adj.[a]
Intracranial volume (in mL)	1401 (139)	1454 (178)	1389 (167)	0.997
Total gray matter	3757 (244)	3656 (224)	3631 (193)	0.009 N[b]-MCI 0.088 N-AD 0.080 MCI-AD 0.896
Total white matter	3384 (160)	3339 (190)	3287 (229)	0.088
Frontal pole	263 (36)	250 (30)	257 (25)	0.074
Frontal ventromedial	19.3 (3.6)	19.1 (3.2)	19.0 (2.6)	0.248
Cingulate anterior	57.8 (11.5)	57.1 (8.9)	57.3 (6.5)	0.887
Temporal pole	101.4 (12.7)	93.6 (15.2)	93.4 (12.5)	0.034 N-MCI 0.023 N-AD 0.066 MCI-AD 0.998
Hippocampus	49.2 (5.6)	44.3 (6.4)	41.7 (5.8)	<0.001 N-MCI <0.001 N-AD <0.001 MCI-AD 0.184
Parahippocampus anterior	32.9 (4.3)	29.2 (5.2)	27.9 (4.6)	<0.001 N-MCI 0.002 N-AD <0.001 MCI-AD 0.467
Cingulate posterior	55.6 (6.5)	51.5 (6.5)	50.5 (7.5)	0.012 N-MCI 0.013 N-AD 0.010 MCI-AD 0.809
Precuneus	106.8 (12.4)	99.6 (14.4)	95.8 (13.7)	0.001 N-MCI 0.036 N-AD 0.006 MCI-AD 0.475
Precentral gyrus	137.5 (18.9)	136.1 (14.6)	138.2 (18.8)	0.922
Postcentral gyrus	105.8 (19.5)	101.7 (15.2)	106.01 (17.4)	0.805
Calcarine cortex	26.3 (4.5)	25.6 (5.4)	24.3 (6.1)	0.180
APL ratio[c]	0.316 (0.048)	0.341 (0.044)	0.357 (0.046)	<0.001 N-MCI 0.027 N-AD 0.002 MCI-AD 0.314
PPL ratio[d]	1.104 (0.128)	1.182 (0.153)	1.249 (0.151)	<0.001 N-MCI 0.033 N-AD 0.001 MCI-AD 0.142

[a] P value of analysis of covariance adjusted for age, gender and years of education.
[b] Normal controls.
[c] Anteroposterior limbic ratio.
[d] Primary-to-posterior limbic ratio.

mean age of 74.8 years (SD = 7.8) and 38/60 (63.3%) females. The accuracy of the models in this sample was as follows: 1) Normal vs. MCI: AUC = 0.798, sensitivity = 0.842, specificity = 0.722. 2) Normal vs. AD: AUC = 0.897, sensitivity = 0.850, specificity = 0.842. 3) Normal vs. Cognitively impaired (MCI plus AD): AUC = 0.762, sensitivity = 0.632, specificity = 0.895. 4) MCI vs. AD: AUC = 0.688, sensitivity = 0.600, specificity = 0.750.

4. Discussion

This study shows that the gray matter volume ratios of preserved to atrophied brain regions in AD may be useful components of the diagnostic models based on MRI-derived volumetric measurements. In particular, the ratios of anterior to posterior limbic structures (APL), and of primary cortex to posterior limbic regions (PPL), were significantly different between normal controls and patients with amnestic MCI or AD. According to a BMA method of variable selection, these ratios were better predictors of the clinical category than the hippocampal and entorhinal volumes in several contexts.

The brain volumes used in this study were calculated with a fully automated method wrapped in a shell script (gm_extractor). The volume estimates obtained with this script were highly reliable in test-retest analyses (r > 0.9). The hippocampal volumes calculated with gm_extractor and those obtained with two previously validated methods (FIRST and SNT) were also highly correlated, but showed significant differences in absolute values (FIRST > gm_extractor >> SNT). These data indicate a difference in measurement scales between gm_extractor and FIRST on one hand, and SNT on the other hand. Suppa et al. reported a similarly high correlation (r = 0.86) between FIRST and SNT, but did not report other measures of agreement [23]. The tendency of the automated methods to inflate brain volumes in comparison to the manual methods seems to be a general class effect, as it has been reported for FIRST, SPM and Freesurfer [19,24,25]. Therefore, the volumes obtained with automated methods may be best understood as the result of specific measurement protocols, akin to operational definitions, and are not directly comparable to the values obtained applying the strict anatomical definitions proper of manual methods. Although manual methods are still considered the gold-standard for brain volumetry, they are time-consuming, require considerable expertise, and depend on strict anatomical definitions, which may be controversial [26]. All these factors act as barriers for their widespread use. Automated methods may be better suited for clinical practice [9], and under certain conditions may be even more accurate (e.g. [27]).

To date, most studies of brain volumetry in patients with amnestic MCI or AD have focused on the medial temporal lobe. Many authors,

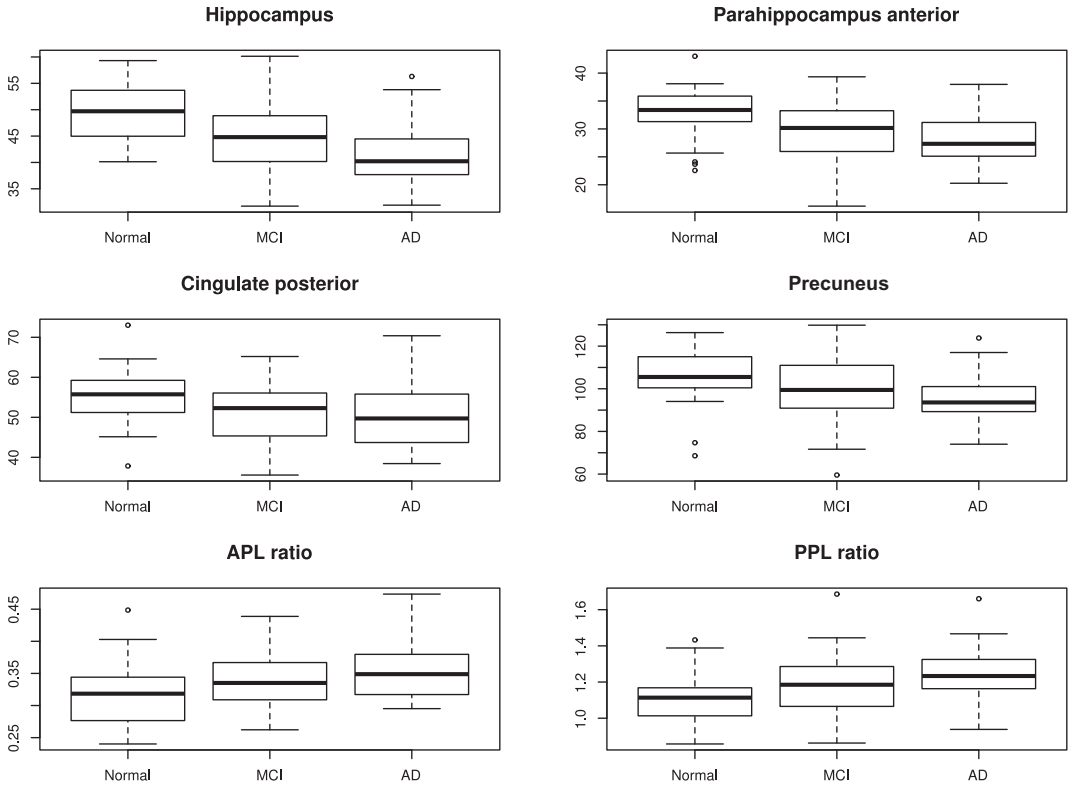

Fig. 3. Boxplots of the normalized volumes of posterior limbic structures and anteroposterior and primary-to-posterior limbic ratios (APL and PPL) according to clinical group.

using manual methods, automated methods or visual scales, have shown a significant reduction of the volumes of the hippocampus and the entorhinal cortex in both AD and MCI patients [28–56]. The atrophy of the hippocampus has been directly related to neuronal loss, and thus can be considered a marker of neurodegeneration [57]. These differences between groups in hippocampal and entorhinal volumes have been extensively used to develop diagnostic models. In a hallmark study, Jack et al. showed the feasibility of performing MR-based volumetric measurements of the temporal lobe [28]. According to their data, the volumes of both the anterior temporal lobe and the hippocampal formation were smaller in AD patients than in normal controls, but the hippocampal volumes provided much better separation between groups. Subsequent studies confirmed the utility of hippocampal volumetry to distinguish between normal controls and AD patients,

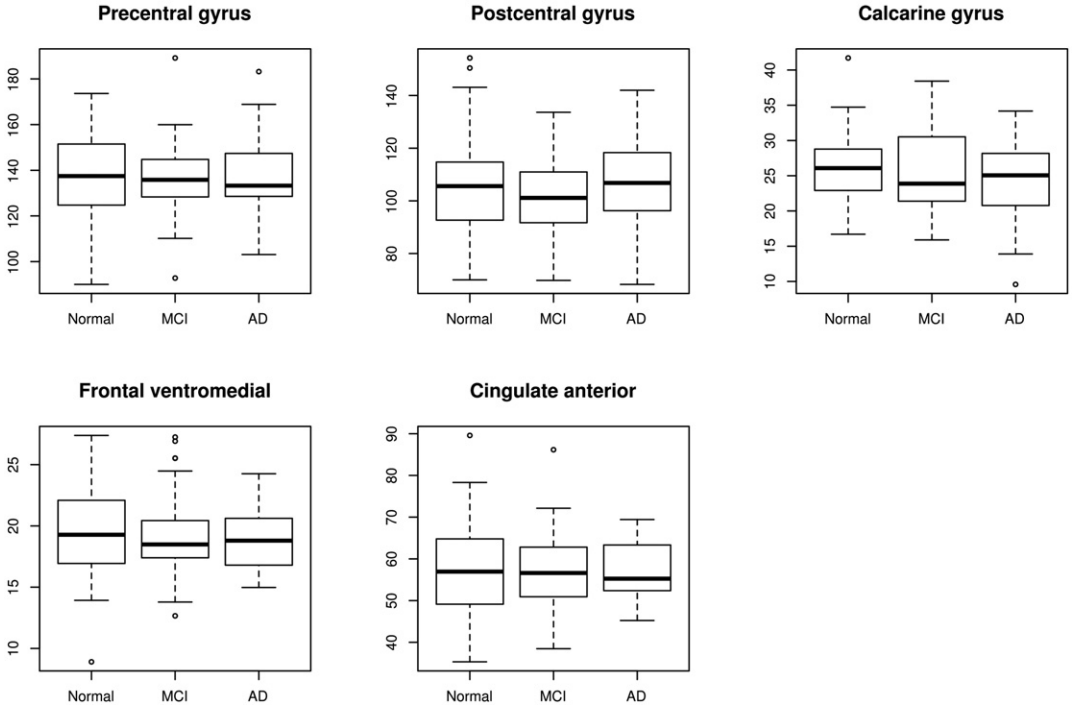

Fig. 4. Boxplots of the normalized volumes of primary cortical regions (upper row) and rostral limbic structures (lower row) according to clinical group.

Table 3
Logistic regression models designed to differentiate the clinical groups in four contexts.

	B	Std. Error (B)	P
Normal vs. MCI			
Constant	2.301	3.453	–
Age	-0.096	0.043	0.016
Gender (Male)	1.144	0.577	0.040
Education	-0.176	0.091	0.028
Cingulate anterior	-0.193	0.055	<0.001
Anteroposterior limbic ratio	5.669[a]	1.415	<0.001
AIC[b] = 95.107			
Normal vs. AD			
Constant	14.553	9.425	–
Age	-0.155	0.084	0.037
Education	-0.308	0.142	0.021
Hippocampus	-0.223	0.088	0.003
Postcentral gyrus	-0.074	0.037	0.027
Primary-to-posterior limbic ratio	1.663[a]	0.681	0.002
AIC = 51.640			
Normal vs. Cog. Impaired (MCI plus AD)			
Constant	2.776	3.178	–
Age	-0.088	0.038	0.014
Education	-0.136	0.074	0.045
Cingulate anterior	-0.189	0.048	<0.001
Anteroposterior limbic ratio	5.321[a]	1.202	<0.001
AIC = 109.960			
MCI vs. AD			
Constant	-4.283	2.046	–
Primary-to-posterior limbic ratio	0.289[a]	0.166	0.044
AIC = 99.379			

[a] Correspond to a change of 0.1 units in the original scale.
[b] Aikake's Information Criterion.

reporting high rates (90–95%) of overall correct classification, sensitivity and specificity [34–36]. As expected, the accuracy of hippocampal volumetry decreased when the study population included patients with MCI. For example, Colliot et al. reported a sensitivity of 75% and a specificity of 70% for the distinction between normal subjects and MCI patients [46], and Chupin et al. reported even lower figures [48]. High-resolution MRI studies have shown significant differences in the pattern of hippocampal atrophy in patients with AD compared to normal controls, opening the door to new-generation methods based on the hippocampal subfields [58] or the hippocampal shape [59]. In a previous work, Suppa et al. described a scaling method quite similar to that used in our APL and PPL ratios, and also based on taking a gray matter volume as reference [56]. In particular, they used a set of standard masks for the computation of the gray matter volumes of the left and right hippocampus, which then were scaled to the patient's total gray matter volume. In addition to diagnostic models, several authors have demonstrated the ability of hippocampal or entorhinal volumetry to predict the progression of MCI to AD (e.g [10–12].). These studies will not be discussed further, as we used a cross-sectional design.

Table 4
Diagnostic accuracy of the logistic regression models designed to differentiate the clinical groups in four contexts.

	Normal vs. MCI	Normal vs. AD	Normal vs. Cog. impaired[a]	MCI vs. AD
AUC[b]	0.830	0.933	0.833	0.620
(CI)[c]	(0.733, 0.910)	(0.859, 0.988)	(0.750, 0.902)	(0.487, 0.753)
Sensitivity	0.740	0.880	0.720	0.600
Specificity	0.800	0.914	0.857	0.630
PPV[d]	0.841	0.880	0.915	0.429
NPV[e]	0.643	0.914	0.588	0.773
LR[f] - positive	3.700	10.267	5.040	1.620
LR - negative	0.325	0.131	0.327	0.635
Cutoff (probability)	0.602	0.425	0.727	0.321

[a] MCI plus AD patients.
[b] Area under the receiver operating characteristic curve.
[c] Bootstrap confidence interval of 95%.
[d] Positive predictive value.
[e] Negative predictive value.
[f] Likelihood ratio.

The utility of other volumetric variables for the diagnosis of MCI and AD has also been explored. In a study with Freesurfer, the most useful variable to discriminate between normal subjects and MCI patients was the temporal cortex (sensitivity = 90%, specificity = 93%) [60]. Other authors showed that the volume of the right amygdala was the most useful variable for AD screening (AUC = 0.972) [61]. A study combining hippocampal volumetry, MR spectroscopy and diffusion-weighted imaging showed that, at 80% specificity, the most sensitive measurement to discriminate MCI from AD was the posterior cingulate gyrus NAA/Cr (67%) [40]. The involvement of other posterior limbic structures in AD is also well-known, but has been less exploited in diagnostic or predictive volumetric models [61–66]. Finally, other authors have reported the potential utility of measuring the volumes of the basal cholinergic system [67] or the corpus callosum [60].

In our study the best model to distinguish normal subjects from patients with MCI included the APL ratio and the anterior cingulate volume. The best model to differentiate normal from cognitively impaired (MCI plus AD) subjects included the same two variables. In both contexts the APL ratio was the variable with the highest posterior probability to be selected by BMA. The AUCs of these models were similar (0.830 and 0.833), and compared favorably to those previously reported. These data indicate that the inclusion of the volumes of posterior limbic structures other than the hippocampus and the entorhinal cortex, by themselves or within composite variables (such as the APL and PPL ratios), might improve the diagnostic accuracy of the resulting models. The inclusion of anterior cingulate volumes in the models exemplifies why it is usually better to avoid bivariate tests for variable selection in multivariable modeling. The best model to discriminate normal from AD subjects included the hippocampal and postcentral volumes, and the PPL ratio. In this context, the hippocampal volume had the highest posterior probability, and the AUC rose to 0.933. Finally, the volumetric variables did not allow an accurate differentiation of MCI from AD patients. This finding may be explained by the characteristics of the ADNI database, which includes patients with MCI at all stages (labeled as early and late MCI), but only early AD cases. Regarding the external validity of the models, their AUCs when applied to the test set were slight lower than those observed in the main (training) sample, except for the MCI vs. AD model. In this context, bootstrap confidence intervals of AUCs can serve as good guides to the future performance of the models in new samples (Table 4). Currently we are planning to investigate the ability of models including the APL and PPL ratios to predict the conversion of MCI to AD, and to combine these variables with other clinical data in the search for better diagnostic tools. In this work we opted not to include the MMSE and FAQ scores in the models in order to reduce the risk of incorporation bias and the overly optimistic results associated with this bias [68].

In conclusion, this study shows that the APL and PPL ratios may be useful components of the models aimed to differentiate normal from MCI and AD patients. These ratios, and other regional gray matter volumes, were easily and reliably calculated with gm_extractor, a fully automated script based on free-software tools.

Conflict of Interest/disclosure statement

AJH and SES have no conflict of interest to report.

Data collection and sharing for this project was funded by the Alzheimer's Disease Neuroimaging Initiative (ADNI) (National Institutes of Health Grant U01 AG024904) and DOD ADNI (Department of Defense award number W81XWH-12-2-0012). ADNI is funded by the National Institute on Aging, the National Institute of Biomedical Imaging and Bioengineering, and through generous contributions from the

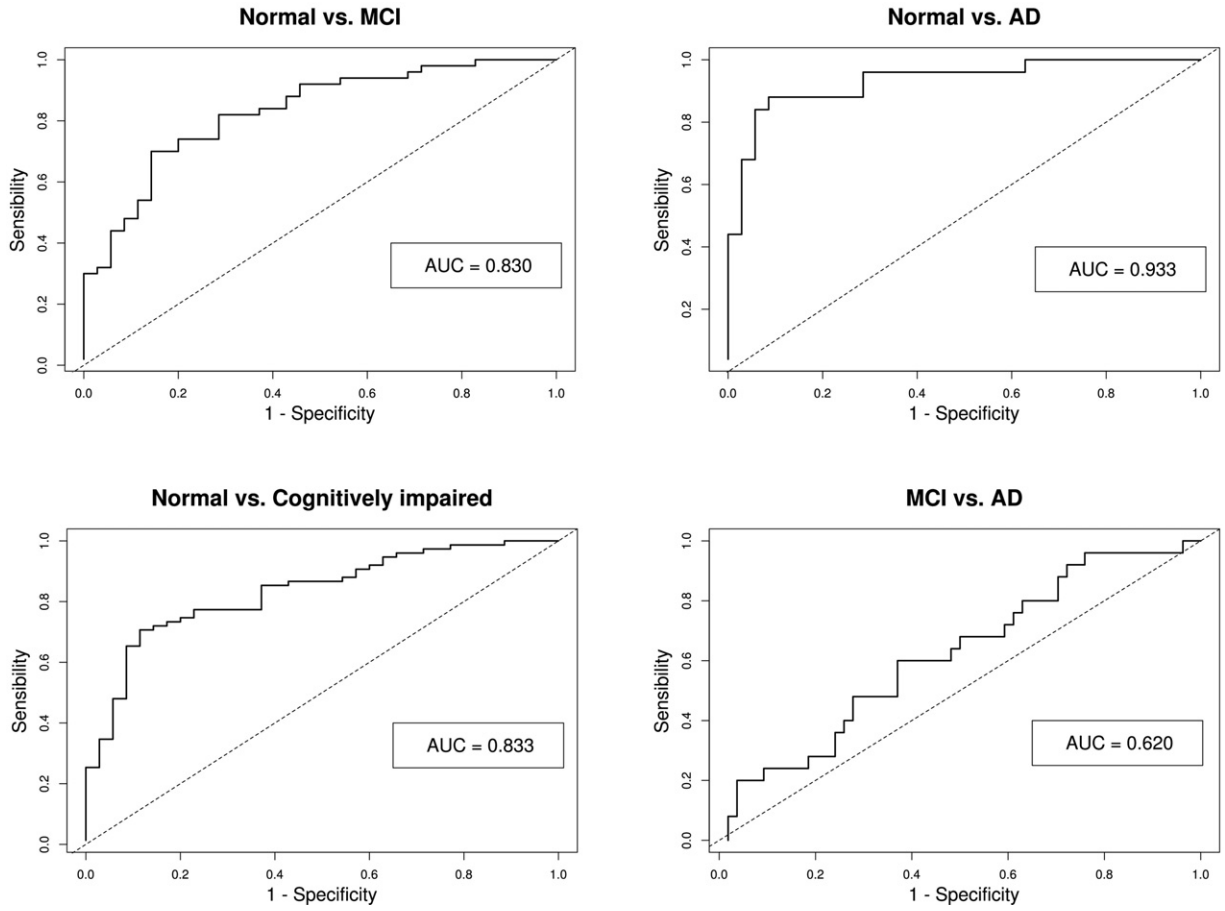

Fig. 5. Receiver operating characteristic (ROC) curves of logistic regression models designed to differentiate the clinical groups in four contexts.

following: AbbVie, Alzheimer's Association; Alzheimer's Drug Discovery Foundation; Araclon Biotech; BioClinica, Inc.; Biogen; Bristol-Myers Squibb Company; CereSpir, Inc.; Cogstate; Eisai Inc.; Elan Pharmaceuticals, Inc.; Eli Lilly and Company; EuroImmun; F. Hoffmann-La Roche Ltd. and its affiliated company Genentech, Inc.; Fujirebio; GE Healthcare; IXICO Ltd.; Janssen Alzheimer Immunotherapy Research & Development, LLC.; Johnson & Johnson Pharmaceutical Research & Development LLC.; Lumosity; Lundbeck; Merck & Co., Inc.; Meso Scale Diagnostics, LLC.; NeuroRx Research; Neurotrack Technologies; Novartis Pharmaceuticals Corporation; Pfizer Inc.; Piramal Imaging; Servier; Takeda Pharmaceutical Company; and Transition Therapeutics. The Canadian Institutes of Health Research is providing funds to support ADNI clinical sites in Canada. Private sector contributions are facilitated by the Foundation for the National Institutes of Health (www.fnih.org). The grantee organization is the Northern California Institute for Research and Education, and the study is coordinated by the Alzheimer's Therapeutic Research Institute at the University of Southern California. ADNI data are disseminated by the Laboratory for Neuro Imaging at the University of Southern California.

References

[1] P. Scheltens, K. Blennow, M.M. Breteler, B. de Strooper, G.B. Frisoni, S. Salloway, W.M. Van der Flier, Alzheimer's disease, Lancet 388 (10043) (2016) 505–517.
[2] B. Winblad, P. Amouyel, S. Andrieu, C. Ballard, C. Brayne, H. Brodaty, A. Cedazo-Minguez, B. Dubois, D. Edvardsson, H. Feldman, L. Fratiglioni, G.B. Frisoni, S. Gauthier, J. Georges, C. Graff, K. Iqbal, F. Jessen, G. Johansson, L. Jönsson, M. Kivipelto, M. Knapp, F. Mangialasche, R. Melis, A. Nordberg, M.O. Rikkert, C. Qiu, T.P. Sakmar, P. Scheltens, L.S. Schneider, R. Sperling, L.O. Tjernberg, G. Waldemar, A. Wimo, H. Zetterberg, Defeating Alzheimer's disease and other dementias: a priority for European science and society, Lancet Neurol. 15 (5) (2016) 455–532.
[3] D.P. Perl, Neuropathology of Alzheimer's disease, Mt Sinai J. Med. 77 (1) (2010) 32–42.
[4] B.A. Vogt, D.M. Finch, C.R. Olson, Functional heterogeneity in cingulate cortex: the anterior executive and posterior evaluative regions, Cereb. Cortex 2 (6) (1992) 435–443.
[5] L. Mosconi, A. Pupi, M.T. De Cristofaro, M. Fayyaz, S. Sorbi, K. Herholz, Functional interactions of the entorhinal cortex: an 18F-FDG PET study on normal aging and Alzheimer's disease, J. Nucl. Med. 45 (3) (2004) 382–392.
[6] K. Hirao, T. Ohnishi, H. Matsuda, K. Nemoto, Y. Hirata, F. Yamashita, T. Asada, T. Iwamoto, Functional interactions between entorhinal cortex and posterior cingulate cortex at the very early stage of Alzheimer's disease using brain perfusion single-photon emission computed tomography, Nucl. Med. Commun. 27 (2) (2006) 151–156.
[7] G.B. Frisoni, M. Pievani, C. Testa, F. Sabattoli, L. Bresciani, M. Bonetti, A. Beltramello, K.M. Hayashi, A.W. Toga, P.M. Thompson, The topography of grey matter involvement in early and late onset Alzheimer's disease, Brain 130 (Pt 3) (2007) 720–730.
[8] O. Devinsky, M.J. Morrell, B.A. Vogt, Contributions of anterior cingulate cortex to behaviour, Brain 118 (Pt 1) (1995) 279–306.
[9] B.G. Rathakrishnan, P.M. Doraiswamy, J.R. Petrella, Science to practice: translating automated brain MRI volumetry in Alzheimer's disease from research to routine diagnostic use in the work-up of dementia, Front. Neurol. 4 (2014) 216.
[10] C.R. Jack Jr., M. Slomkowski, S. Gracon, T.M. Hoover, J.P. Felmlee, K. Stewart, Y. Xu, M. Shiung, P.C. O'Brien, R. Cha, D. Knopman, R.C. Petersen, MRI as a biomarker of disease progression in a therapeutic trial of milameline for AD, Neurology 60 (2) (2003) 253–260.
[11] A.T. Du, N. Schuff, X.P. Zhu, W.J. Jagust, B.L. Miller, B.R. Reed, J.H. Kramer, D. Mungas, K. Yaffe, H.C. Chui, M.W. Weiner, Atrophy rates of entorhinal cortex in AD and normal aging, Neurology 60 (3) (2003) 481–486.
[12] V.A. Cardenas, A.T. Du, D. Hardin, F. Ezekiel, P. Weber, W.J. Jagust, H.C. Chui, N. Schuff, M.W. Weiner, Comparison of methods for measuring longitudinal brain change in cognitive impairment and dementia, Neurobiol. Aging 24 (4) (2003) 537–544.
[13] M. Jenkinson, C.F. Beckmann, T.E. Behrens, M.W. Woolrich, S.M. Smith, FSL, NeuroImage 62 (2012) 782–790.
[14] R.C. Petersen, Mild cognitive impairment, Continuum (Minneap Minn) 22 (2 Dementia) (2016) 404–418.
[15] E.S. Lutkenhoff, M. Rosenberg, J. Chiang, K. Zhang, J.D. Pickard, A.M. Owen, M.M. Monti, Optimized brain extraction for pathological brains (optiBET), PLoS One 9 (12) (2014) e115551.
[16] R Core Team, R: A Language and Environment for Statistical Computing, R Foundation for Statistical Computing, Vienna, Austria, 2016 https://www.R-project.org/.
[17] B. Patenaude, S.M. Smith, D. Kennedy, M. Jenkinson, A Bayesian model of shape and appearance for subcortical brain, NeuroImage 56 (3) (2011) 907–922.

[18] Y.Y. Hsu, N. Schuff, A.T. Du, K. Mark, X. Zhu, D. Hardin, M.W. Weiner, Comparison of automated and manual MRI volumetry of hippocampus in normal aging and dementia, J. Magn. Reson. Imaging 16 (3) (2002) 305–310.
[19] F.L. Seixas, D.C. Muchaluat Saade, A. Conci, A. Silveira de Souza, F. Tovar-Moll, I. Bramatti, Anatomical brain MRI segmentation methods: volumetric assessment of the hippocampus, IWSSIP 2010-17th International Conference on Systems, Signals and Image Processing 2010, pp. 247–251http://www2.ic.uff.br/iwssip2010/Proceedings/nav/papers/paper_78.pdf.
[20] A. Rafteryh, J. Hoeting, C. Volinsky, I. Painter, K.Y. Yeung, BMA: Bayesian Model Averaging. R Package Version 3.18.6.2015, https://CRAN.R-project.org/package=BMA.
[21] M. Lopez-Raton, M.X. Rodriguez-Alvarez, C. Cadarso, F. Gude, Optimal cutpoints: an R package for selecting optimal cutpoints in diagnostic tests, J. Stat. Softw. 61 (8) (2014) 1–36.
[22] A. Canty, B. Ripley, boot: Bootstrap R (S-Plus) Functions. R Package Version 1.3-18, 2016.
[23] P. Suppa, H. Hampel, T. Kepp, C. Lange, L. Spies, J.B. Fiebach, B. Dubois, R. Buchert, Alzheimer's disease neuroimaging initiative: performance of hippocampus volumetry with FSL-FIRST for prediction of Alzheimer's disease dementia in at risk subjects with amnestic mild cognitive impairment, J. Alzheimers Dis. 51 (3) (2016) 867–873.
[24] I. Fellhauer, F.G. Zöllner, J. Schröder, C. Degen, L. Kong, M. Essig, P.A. Thomann, L.R. Schad, Comparison of automated brain segmentation using a brain phantom and patients with early Alzheimer's dementia or mild cognitive impairment, Psychiatry Res. 233 (3) (2015) 299–305.
[25] G. Sánchez-Benavides, B. Gómez-Ansón, A. Sainz, Y. Vives, M. Delfino, J. Peña-Casanova, Manual validation of FreeSurfer's automated hippocampal segmentation in normal aging, mild cognitive impairment, and Alzheimer disease subjects, Psychiatry Res. 181 (3) (2010) 219–225.
[26] C.R. Jack Jr., F. Barkhof, M.A. Bernstein, M. Cantillon, P.E. Cole, C. Decarli, B. Dubois, S. Duchesne, N.C. Fox, G.B. Frisoni, H. Hampel, D.L. Hill, K. Johnson, J.F. Mangin, P. Scheltens, A.J. Schwarz, R. Sperling, J. Suhy, P.M. Thompson, M. Weiner, N.L. Foster, Steps to standardization and validation of hippocampal volumetry as a biomarker in clinical trials and diagnostic criterion for Alzheimer's disease, Alzheimers Dement. 7 (4) (2011) 474–485.
[27] M. Menéndez González, E. Suárez-Sanmartin, C. García, P. Martínez-Camblor, E. Westman, A. Simmons, Manual planimetry of the medial temporal lobe versus automated volumetry of the hippocampus in the diagnosis of Alzheimer's disease, Cureus 8 (3) (2016) e544.
[28] C.R. Jack Jr., R.C. Petersen, P.C. O'Brien, E.G. Tangalos, MR-based hippocampal volumetry in the diagnosis of Alzheimer's disease, Neurology 42 (1) (1992) 183–188.
[29] L. Parnetti, D.T. Lowenthal, O. Presciutti, G.P. Pelliccioli, R. Palumbo, G. Gobbi, P. Chiarini, B. Palumbo, R. Tarducci, U. Senin, 1H-MRS, MRI-based hippocampal volumetry, and 99mTc-HMPAO-SPECT in normal aging, age-associated memory impairment, and probable Alzheimer's disease, J. Am. Geriatr. Soc. 44 (2) (1996) 133–138.
[30] M.P. Laakso, K. Partanen, P. Riekkinen, M. Lehtovirta, E.L. Helkala, M. Hallikainen, T. Hanninen, P. Vainio, H. Soininen, Hippocampal volumes in Alzheimer's disease, Parkinson's disease with and without dementia, and in vascular dementia: an MRI study, Neurology 46 (3) (1996) 678–681.
[31] M.J. de Leon, A. Convit, S. DeSanti, M. Bobinski, A.E. George, H.M. Wisniewski, H. Rusinek, R. Carroll, L.A. Saint Louis, Contribution of structural neuroimaging to the early diagnosis of Alzheimer's disease, Int. Psychogeriatr. 9 (Suppl. 1) (1997) 183–190 (discussion 247–52).
[32] E. Mori, Y. Yoneda, H. Yamashita, N. Hirono, M. Ikeda, A. Yamadori, Medial temporal structures relate to memory impairment in Alzheimer's disease: an MRI volumetric study, J. Neurol. Neurosurg. Psychiatry 63 (2) (1997) 214–221.
[33] S. Köhler, S.E. Black, M. Sinden, C. Szekely, D. Kidron, J.L. Parker, J.K. Foster, M. Moscovitch, G. Winocour, J.P. Szalai, M.J. Bronskill, Memory impairments associated with hippocampal versus parahippocampal-gyrus atrophy: an MR volumetry study in Alzheimer's disease, Neuropsychologia 36 (9) (1998) 901–914.
[34] M.P. Laakso, H. Soininen, K. Partanen, M. Lehtovirta, M. Hallikainen, T. Hänninen, E.L. Helkala, P. Vainio, P.J. Riekkinen Sr., MRI of the hippocampus in Alzheimer's disease: sensitivity, specificity, and analysis of the incorrectly classified subjects, Neurobiol. Aging 19 (1) (1998) 23–31.
[35] K. Juottonen, M.P. Laakso, K. Partanen, H. Soininen, Comparative MR analysis of the entorhinal cortex and hippocampus in diagnosing Alzheimer disease, AJNR Am. J. Neuroradiol. 20 (1) (1999) 139–144.
[36] M. Golebiowski, M. Barcikowska, A. Pfeffer, Magnetic resonance imaging-based hippocampal volumetry in patients with dementia of the Alzheimer type, Dement. Geriatr. Cogn. Disord. 10 (4) (1999) 284–288.
[37] L.O. Wahlund, P. Julin, J. Lindqvist, P. Scheltens, Visual assessment of medical temporal lobe atrophy in demented and healthy control subjects: correlation with volumetry, Psychiatry Res. 90 (3) (1999) 193–199.
[38] R.C. Petersen, C.R. Jack Jr., Y.C. Xu, S.C. Waring, P.C. O'Brien, G.E. Smith, R.J. Ivnik, E.G. Tangalos, B.F. Boeve, E. Kokmen, Memory and MRI-based hippocampal volumes in aging and AD, Neurology 54 (3) (2000) 581–587.
[39] M.S. Mega, G.W. Small, M.L. Xu, J. Felix, M. Manese, N.P. Tran, J.I. Dailey, L.M. Ercoli, S.Y. Bookheimer, A.W. Toga, Hippocampal atrophy in persons with age-associated memory impairment: volumetry within a common space, Psychosom. Med. 64 (3) (2002) 487–492.
[40] K. Kantarci, Y. Xu, M.M. Shiung, P.C. O'Brien, R.H. Cha, G.E. Smith, R.J. Ivnik, B.F. Boeve, S.D. Edland, E. Kokmen, E.G. Tangalos, R.C. Petersen, C.R. Jack Jr., Comparative diagnostic utility of different MR modalities in mild cognitive impairment and Alzheimer's disease, Dement. Geriatr. Cogn. Disord. 14 (4) (2002) 198–207.
[41] C. Testa, M.P. Laakso, F. Sabattoli, R. Rossi, A. Beltramello, H. Soininen, G.B. Frisoni, A comparison between the accuracy of voxel-based morphometry and hippocampal volumetry in Alzheimer's disease, J. Magn. Reson. Imaging 19 (3) (2004) 274–282.
[42] M.J. Müller, D. Greverus, P.R. Dellani, C. Weibrich, P.R. Wille, A. Scheurich, P. Stoeter, A. Fellgiebel, Functional implications of hippocampal volume and diffusivity in mild cognitive impairment, NeuroImage 28 (4) (2005) 1033–1042.
[43] L. Bresciani, R. Rossi, C. Testa, C. Geroldi, S. Galluzzi, M.P. Laakso, A. Beltramello, H. Soininen, G.B. Frisoni, Visual assessment of medial temporal atrophy on MR films in Alzheimer's disease: comparison with volumetry, Aging Clin. Exp. Res. 17 (1) (2005) 8–13.
[44] K. Ishii, T. Soma, A.K. Kono, H. Sasaki, N. Miyamoto, T. Fukuda, K. Murase, Automatic volumetric measurement of segmented brain structures on magnetic resonance imaging, Radiat. Med. 24 (6) (2006) 422–430.
[45] F.L. Giesel, P.A. Thomann, H.K. Hahn, M. Politi, B. Stieltjes, M.A. Weber, J. Pantel, I.D. Wilkinson, P.D. Griffiths, J. Schröder, M. Essig, Comparison of manual direct and automated indirect measurement of hippocampus using magnetic resonance imaging, Eur. J. Radiol. 66 (2) (2008) 268–273.
[46] O. Colliot, G. Chételat, M. Chupin, B. Desgranges, B. Magnin, H. Benali, B. Dubois, L. Garnero, F. Eustache, S. Lehéricy, Discrimination between Alzheimer disease, mild cognitive impairment, and normal aging by using automated segmentation of the hippocampus, Radiology 248 (1) (2008) 194–201.
[47] A.M. Jauhiainen, M. Pihlajamäki, S. Tervo, E. Niskanen, H. Tanila, T. Hänninen, R.L. Vanninen, H. Soininen, Discriminating accuracy of medial temporal lobe volumetry and fMRI in mild cognitive impairment, Hippocampus 19 (2) (2009) 166–175.
[48] M. Chupin, E. Gérardin, R. Cuingnet, C. Boutet, L. Lemieux, S. Lehéricy, H. Benali, L. Garnero, O. Colliot, Alzheimer's disease neuroimaging initiative: fully automatic hippocampus segmentation and classification in Alzheimer's disease and mild cognitive impairment applied on data from ADNI, Hippocampus 19 (6) (2009) 579–587.
[49] A. Cherubini, P. Péran, I. Spoletini, M. Di Paola, F. Di Iulio, G.E. Hagberg, G. Sancesario, W. Gianni, P. Bossù, C. Caltagirone, U. Sabatini, G. Spalletta, Combined volumetry and DTI in subcortical structures of mild cognitive impairment and Alzheimer's disease patients, J. Alzheimers Dis. 19 (4) (2010) 1273–1282.
[50] H.K. Mak, Z. Zhang, K.K. Yau, L. Zhang, Q. Chan, L.W. Chu, Efficacy of voxel-based morphometry with DARTEL and standard registration as imaging biomarkers in Alzheimer's disease patients and cognitively normal older adults at 3.0 Tesla MR imaging, J. Alzheimers Dis. 23 (4) (2011) 655–664.
[51] L. Cavallin, L. Bronge, Y. Zhang, A.R. Oksengård, L.O. Wahlund, L. Fratiglioni, R. Axelsson, Comparison between visual assessment of MTA and hippocampal volumes in an elderly, non-demented population, Acta Radiol. 53 (5) (2012) 573–579.
[52] C. Boutet, M. Chupin, O. Colliot, M. Sarazin, G. Mutlu, A. Drier, A. Pellot, D. Dormont, S. Lehéricy, Alzheimer's disease neuroimaging initiative: is radiological evaluation as good as computer-based volumetry to assess hippocampal atrophy in Alzheimer's disease? Neuroradiology 54 (12) (2012) 1321–1330.
[53] L. Ferrarini, B. van Lew, J.H. Reiber, C. Gandin, L. Galluzzo, E. Scafato, G.B. Frisoni, J. Milles, M. Pievani, IPREA working group (Italian Project on epidemiology of Alzheimer's disease): hippocampal atrophy in people with memory deficits: results from the population-based IPREA study, Int. Psychogeriatr. 26 (7) (2014) 1067–1081.
[54] S.H. Han, M.A. Lee, S.S. An, S.W. Ahn, Y.C. Youn, K.Y. Park, Diagnostic value of Alzheimer's disease-related individual structural volume measurements using IBASPM, J. Clin. Neurosci. 21 (12) (2014) 2165–2169.
[55] W.B. Jung, Y.M. Lee, Y.H. Kim, C.W. Mun, Automated classification to predict the progression of Alzheimer's disease using whole-brain Volumetry and DTI, Psychiatry Investig. 12 (1) (2015) 92–102.
[56] P. Suppa, U. Anker, L. Spies, I. Bopp, B. Rüegger-Frey, R. Klaghofer, C. Gocke, H. Hampel, S. Beck, R. Buchert, Fully automated atlas-based hippocampal volumetry for detection of Alzheimer's disease in a memory clinic setting, J. Alzheimers Dis. 44 (1) (2015) 183–193.
[57] J.J. Kril, J. Hodges, G. Halliday, Relationship between hippocampal volume and CA1 neuron loss in brains of humans with and without Alzheimer's disease, Neurosci. Lett. 361 (1–3) (2004) 9–12.
[58] S.G. Mueller, M.W. Weiner, Selective effect of age, Apo e4, and Alzheimer's disease on hippocampal subfields, Hippocampus 19 (6) (2009) 558–564.
[59] E. Gerardin, G. Chételat, M. Chupin, R. Cuingnet, B. Desgranges, H.S. Kim, M. Niethammer, B. Dubois, S. Lehéricy, L. Garnero, F. Eustache, O. Colliot, Alzheimer's disease neuroimaging initiative: multidimensional classification of hippocampal shape features discriminates Alzheimer's disease and mild cognitive impairment from normal aging, NeuroImage 47 (4) (2009) 1476–1486.
[60] T. Nesteruk, M. Nesteruk, M. Styczyńska, M. Barcikowska-Kotowicz, J. Walecki, Radiological evaluation of strategic structures in patients with mild cognitive impairment and early Alzheimer's disease, Pol. J. Radiol. 81 (2016) 288–294.
[61] C. Luckhaus, M. Jänner, M. Cohnen, M.O. Flüss, S.J. Teipel, M. Grothe, H. Hampel, J. Kornhuber, E. Rüther, O. Peters, T. Supprian, W. Gaebel, U. Mödder, H.J. Wittsack, A novel MRI-biomarker candidate for Alzheimer's disease composed of regional brain volume and perfusion variables, Eur. J. Neurol. 17 (12) (2010) 1437–1444.
[62] D.J. Callen, S.E. Black, F. Gao, C.B. Caldwell, J.P. Szalai, Beyond the hippocampus: MRI volumetry confirms widespread limbic atrophy in AD, Neurology 57 (9) (2001) 1669–1674.
[63] S.Y. Ryu, M.J. Kwon, S.B. Lee, D.W. Yang, T.W. Kim, I.U. Song, P.S. Yang, H.J. Kim, A.Y. Lee, Measurement of precuneal and hippocampal volumes using magnetic resonance volumetry in Alzheimer's disease, J. Clin. Neurol. 6 (4) (2010) 196–203.
[64] F. Palesi, P. Vitali, P. Chiarati, G. Castellazzi, E. Caverzasi, A. Pichiecchio, E. Colli-Tibaldi, F. D'Amore, I. D'Errico, E. Sinforiani, S. Bastianello, DTI and MR Volumetry of hippocampus-PC/PCC circuit: in search of early micro- and macrostructural signs of Alzheimer's disease, Neurol. Res. Int. 2012 (2012) 517876.

[65] L. Clerx, H.I. Jacobs, S. Burgmans, E.H. Gronenschild, H.B. Uylings, C. Echávarri, P.J. Visser, F.R. Verhey, P. Aalten, Sensitivity of different MRI-techniques to assess gray matter atrophy patterns in Alzheimer's disease is region-specific, Curr. Alzheimer Res. 10 (9) (2013) 940–951.
[66] H.K. Mak, W. Qian, K.S. Ng, Q. Chan, Y.Q. Song, L.W. Chu, K.K. Yau, Combination of MRI hippocampal volumetry and arterial spin labeling MR perfusion at 3-Tesla improves the efficacy in discriminating Alzheimer's disease from cognitively normal elderly adults, J. Alzheimers Dis. 41 (3) (2014) 749–758.
[67] M. Grothe, H. Heinsen, S. Teipel, Longitudinal measures of cholinergic forebrain atrophy in the transition from healthy aging to Alzheimer's disease, Neurobiol. Aging 34 (4) (2013) 1210–1220.
[68] T.B. Newman, M.A. Kohn, Evidence-based Diagnosis, Cambridge University Press, Cambridge, UK, 2009 99.